

CRITICAL LOAD-CASE AND CONSTRAINT IDENTIFICATION FOR PRELIMINARY COMPOSITE WING SIZING USING RAPID DESIGN TOOLS

Yingjun Pan[1] & Mushfiqul Alam[1]
[1] Centre for Aeronautics, Faculty of Engineering and Applied Science (FEAS), Cranfield University, United Kingdom
Y.Pan@cranfield.ac.uk, mushfiqul.alam@cranfield.ac.uk

Abstract

Preliminary composite wing sizing requires early identification of the load cases and structural constraints that govern mass, stiffness, and aeroelastic behaviour. Although detailed aircraft design requires the assessment of many manoeuvre, gust, ground, landing, and localised loading conditions, such an exhaustive load set is not practical during early multidisciplinary design optimisation. This paper presents a rapid methodology for identifying critical load cases and governing constraints for preliminary composite wing sizing using the Structural Layout Tool and Structural Analysis Tool framework. The approach is demonstrated using a composite wing-box model based on the NASA Common Research Model. A reduced set of representative aerodynamic, gust, and engine-induced load cases is defined, including cruise, symmetric pull-up, push-down, flap-down, rolling manoeuvre, discrete gust, and engine loading conditions. Structural sizing is performed using coarse 7-section and refined 33-section spanwise discretisation to assess the influence of model resolution. The resulting wing models are compared in terms of structural mass, spanwise thickness distribution, static deflection, elastic twist, gust response, modal behaviour, and flutter speed. Sensitivity studies are used to quantify the influence of strength, buckling, fatigue, secondary-structure and fuel inertia, and engine effects on the final sized structure. The results show that sizing based only on a conventional 2.5 g symmetric pull-up strength case is insufficient for reliable preliminary composite wing design. Buckling constraints strongly influence panel sizing, stiffness, and flutter margin, while fatigue and inertial effects modify local sizing and structural response. Engine-induced loads are locally important near the pylon attachment region, whereas lumped engine mass has a significant effect on modal characteristics and flutter speed. The refined 33-section model improves the representation of local load paths and torsional stiffness variation, while the 7-section model remains useful for rapid global screening. The proposed methodology provides a practical basis for reducing preliminary sizing load sets while retaining the dominant structural and aeroelastic design drivers.

Keywords: preliminary aircraft design; composite wing sizing; load-case criticality; structural optimisation; aeroelasticity; multidisciplinary design optimisation.

1 Introduction

The development of next-generation aircraft requires structural design methodologies that can support rapid decision-making while maintaining sufficient physical fidelity. Increasing pressure to reduce fuel burn, emissions, and operating cost has led to greater emphasis on lightweight airframe structures, higher-aspect-ratio wings, advanced composite materials, and multidisciplinary design optimisation (MDO) [1], [2]. These developments increase the coupling between aerodynamic loading, structural stiffness, mass distribution, and aeroelastic stability, making the early identification of governing design drivers essential during preliminary design.

Aircraft wing sizing is traditionally driven by a combination of strength, stiffness, fatigue, and aeroelastic requirements. In detailed design and certification, a large number of load cases must be assessed, including manoeuvre loads, gust loads, ground loads, landing loads, engine loads, and localised structural loads [3], [4]. However, the direct use of extensive certification-style load sets during preliminary design is computationally inefficient and can obscure the key design drivers that determine the structural layout. At the same time, relying on a small number of conventional load cases, such as the 2.5 g symmetric pull-up manoeuvre, may result in an incomplete assessment of governing constraints and may lead either to under-designed or overly conservative preliminary

https://doi.org/10.71945/icas2026_0628

structures.
Preliminary MDO therefore requires a balanced approach. The load set must be small enough to allow rapid iteration across many candidate designs, but sufficiently representative to capture the internal load paths, structural constraints, and aeroelastic effects that influence final sizing. This requirement is particularly important for composite wings, where stiffness tailoring, laminate thickness, buckling resistance, and aeroelastic response are strongly coupled [5], [6], [7]. A systematic method is therefore needed to identify which load cases and constraints are critical at the early design stage, and how their inclusion affects structural mass, stiffness, deformation, and flutter characteristics.
Recent work has demonstrated rapid preliminary wing sizing using the Structural Layout Tool (SLoT) and Structural Analysis Tool (SAIT), including metallic and composite wing-box sizing, aeroelastic assessment, sensitivity analysis, and data-driven MDO applications [8]. The present paper builds on that broader framework but addresses a narrower and more practically focused question: how can critical load cases and active structural constraints be identified and prioritised for preliminary composite wing sizing?
The methodology is demonstrated using a composite wing based on the NASA Common Research Model (CRM), which provides a representative long-range transport aircraft configuration and has been widely used for aerodynamic verification, validation, and aerostructural studies [9], [10], [11]. A reduced set of representative load cases is defined, including cruise, buffet, symmetric pull-up, symmetric push-down, flap-down landing, rolling manoeuvre, discrete gust, and engine-induced loading conditions. These cases are used to size and assess parametric composite wing-box models within the SLoT–SAIT environment.
The influence of spanwise model resolution is examined by comparing a coarse 7-section representation with a refined 33-section wing-box model. The sized models are assessed in terms of mass distribution, component thickness, static deformation, elastic twist, gust response, modal behaviour, and flutter speed. Sensitivity studies are then used to determine how the inclusion of buckling, fatigue, secondary structural mass, fuel mass, engine loading, and lumped engine mass representation changes the predicted structural and aeroelastic behaviour.
The main contribution of this paper is the formulation and demonstration of a practical criticality-identification process for preliminary composite wing sizing. Rather than presenting a general rapid sizing framework, the paper focuses on how structural mass, stiffness, and aeroelastic margins change as additional load cases and constraints are progressively introduced. This enables the governing design drivers to be identified and provides guidance on which load cases and constraints should be retained during early-stage MDO studies.
The specific objectives of this work are to:

1. define a representative reduced load-case set for preliminary composite wing sizing;
2. assess the effect of model discretisation on mass, stiffness, and aeroelastic predictions;
3. quantify the influence of buckling, fatigue, secondary structural components, fuel, and engine-related effects on the sized wing;
4. identify the load cases and constraints that govern structural mass, static deformation, and flutter behaviour; and
5. provide recommendations for using rapid design tools in preliminary MDO workflows.

The remainder of the paper is organised as follows. Section 2 describes the rapid structural and aeroelastic sizing framework and introduces the CRM composite wing model used in the study. Section 3 defines the selected load cases, sizing constraints, and criticality-identification process. Section 4 presents and discusses the sizing results, including the effects of model resolution, load cases, and constraints on structural mass, static response, gust response, and flutter behaviour. Finally, Section 5 presents the conclusions and outlines future work.

2 Rapid Structural and Aeroelastic Sizing Framework

The present study uses the Structural Layout Tool (SLoT) and Structural Analysis Tool (SAIT) framework for rapid preliminary structural and aeroelastic assessment of wing-box configurations. The full development of the toolset, including the structural idealisation, sizing procedure,

https://doi.org/10.71945/icas2026_0628

optimisation workflow, and aeroelastic analysis capability, has been described previously [8], [12]. Therefore, only a brief overview is provided here, with emphasis on how the framework is used in this paper to identify critical load cases and governing constraints.

Figure 1 illustrates the overall SLoT–SAIT workflow used for preliminary aerostructural sizing, facilitating the conceptional design to the detail design. The process begins with aircraft-level design inputs, including wing geometry, mass properties, material system, secondary structural components, and selected flight or engine load cases. Aerodynamic load analysis is then performed to generate spanwise lift, shear force, bending moment, and torque distributions. These loads are passed to the structural sizing modules, where the wing box is represented using stiffened skin-stringer panels, spars, ribs, and equivalent laminate properties for composite components.

The sizing process seeks a minimum-mass wing-box design while satisfying structural and aeroelastic constraints. These include strength, buckling, fatigue, stiffness, divergence, and flutter requirements. The sized structure is subsequently assessed in terms of mass distribution, component thickness, static deflection, elastic twist, modal characteristics, gust response, and flutter speed. This enables different load cases and constraint combinations to be compared on a consistent basis.

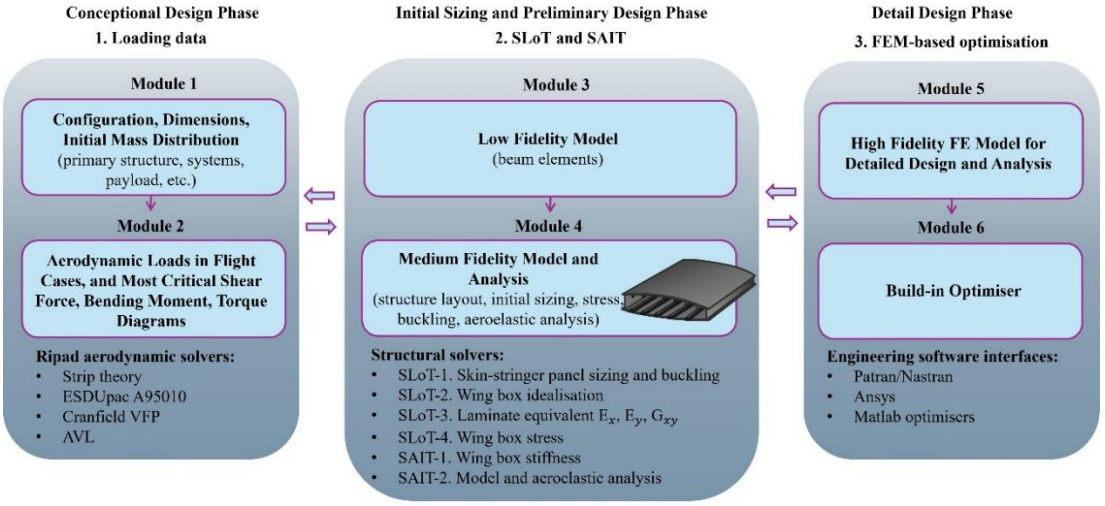


Figure 1. Schematic of the SLoT–SAIT workflow used for rapid preliminary wing sizing and aeroelastic assessment. The workflow links aerodynamic load generation, structural sizing, constraint evaluation, and aeroelastic analysis within an iterative preliminary de design environment. Full details of the tool development and validation are given in Ref [8].

In this paper, the SLoT–SAIT framework is used as a criticality-identification tool rather than as the main research contribution itself. A baseline structural sizing case is first established using a conventional 2.5 g symmetric pull-up manoeuvre. Additional design inputs are then introduced progressively, including buckling constraints, aeroelastic requirements, wing-box inertial loads, secondary structural masses, fuel mass, fatigue loading, push-down manoeuvres, flap-down landing loads, rolling manoeuvres, and engine-induced loads.

For each sizing step, the resulting wing model is evaluated using the same set of structural and aeroelastic metrics. The effect of each additional load case or constraint is quantified by comparing the resulting mass, stiffness, static deformation, twist, gust response, modal behaviour, and flutter speed with the baseline case. In this way, the methodology identifies not only the load cases producing the largest applied loads on the wing, but also those that most strongly influence the final sized structure. This distinction is important for preliminary multidisciplinary design optimisation. Some load cases may be globally critical because they increase total structural mass or reduce aeroelastic margins. Others may be locally critical because they drive reinforcement in specific regions, such as the engine attachment or high-lift-device regions. The proposed approach therefore supports the selection of a reduced but representative set of load cases for early-stage composite wing sizing, avoiding both excessive certification-level load enumeration and overly simplified sizing based on a single manoeuvre condition.

3 CRM Wing Case Study and Structural Model

3.1 Reference aircraft configuration

The methodology is demonstrated using a wing model based on the NASA Common Research Model (CRM). The CRM represents a long-range, twin-aisle transport aircraft configuration and has been widely used as a reference geometry for aerodynamic verification, validation, and aerostructural studies [13], [14] . The configuration includes the fuselage, wing, horizontal tailplane, engine nacelles, and pylons. In the present study, the focus is placed on the structural sizing and aeroelastic assessment of the wing-box structure. The main aircraft and wing parameters are summarised in Table 1, with selected parameters referenced from the Boeing 777-200ER due to its similarity to the CRM configuration [15].

Table 1 CRM specifications.

Parameter	Value	Parameter	Value
Wing aspect ratio	9	Maximum take-off weight (MTOW, kg)	297500
Wing reference surface area (m^2)	383.69	Maximum landing weight (MLW, kg)	213180
Wing semi-span (m)	29.38	Maximum zero fuel weight (MZFW, kg)	195040
Mean aerodynamic chord (m)	7.01	Operational empty weight (OEW, kg)	138100
Quarter-chord sweep angle (°)	35	Reserve fuel (kg)	15000
Cruise Mach number	0.85	Engine mass (kg)	7320
Cruise lift coefficient	0.5	Take-off Thrust (kN)	417
Initial cruise altitude (ft)	37000	Maximum cruise thrust (kN)	95

3.2 Wing structural model

The structural model consists of the inner and outer wing-box regions, which form the primary load-carrying structure of the wing. The wing box is bounded by the front and rear spars and is divided spanwise according to the rib locations. The outer wing is represented by two-spar wing-box sections, while the inner wing includes an additional middle spar to account for the structural arrangement near the inboard region and engine/pylon location.

The primary structural components include the upper and lower skin covers, front and rear spar webs, rib webs, spar caps, stringers, rib flanges, and web stiffeners. The engine and pylon are located near the wing kink region, where localised engine-induced loads are introduced in the load-case analysis. Cut-outs, manholes, and detailed local structural features are not included, since the objective of the study is preliminary sizing and critical load-case identification rather than detailed component-level stress assessment.

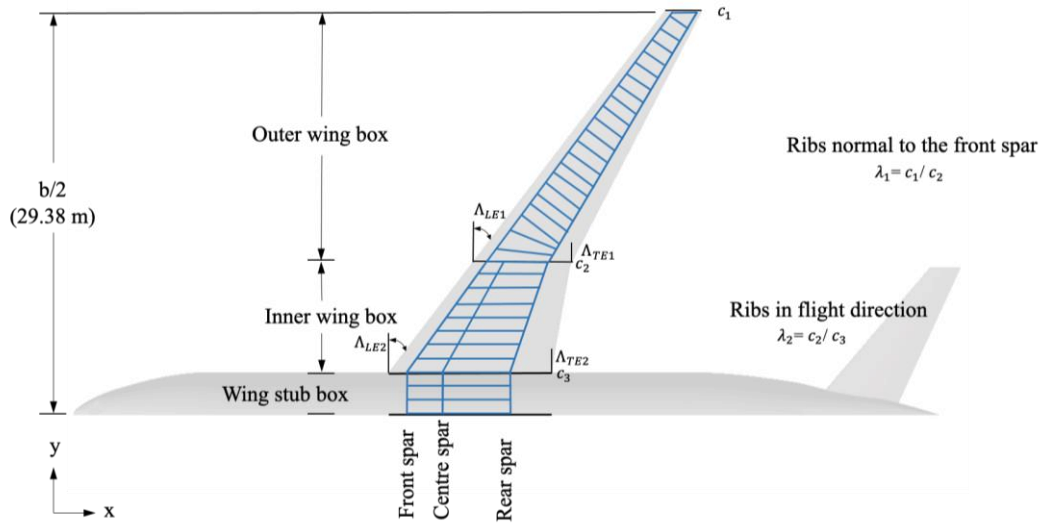


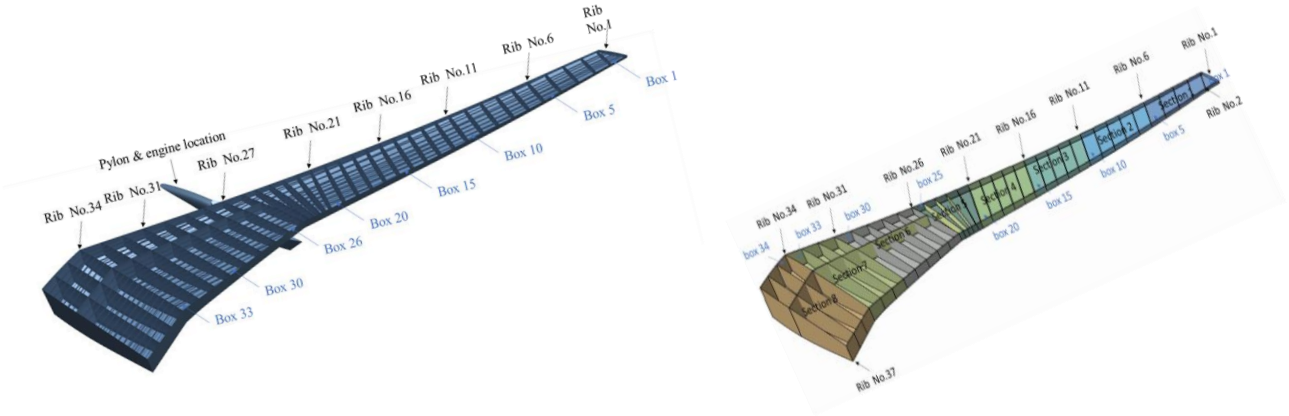
Figure 2. Aircraft outer shape and wing structural layout.

3.3 Spanwise discretisation for sizing

Two levels of spanwise structural discretisation are considered to assess the effect of model resolution on the identification of critical load cases and constraints, shown in Figure 3. The refined model divides the wing into 33 rib-bounded wing-box sections from tip to root. In this representation, each section

https://doi.org/10.71945/icas2026_0628

can be sized independently, allowing local load variations and stiffness changes to be captured with greater resolution. A coarser 7-section model is also considered. In this model, several adjacent wing-box sections are grouped into larger design regions, and uniform panel thicknesses and stringer dimensions are applied within each region. This reduces the number of sizing variables and improves computational efficiency, but it may also introduce conservative sizing where a large region is governed by a local critical condition. The comparison between the 7-section and 33-section models is used to determine whether a coarse model is sufficient for preliminary load-case screening, and when a refined model becomes necessary to represent localised effects such as engine loading, high-lift-device loading, and spanwise stiffness variation.



(a) 33 – Section (b) 7 - section

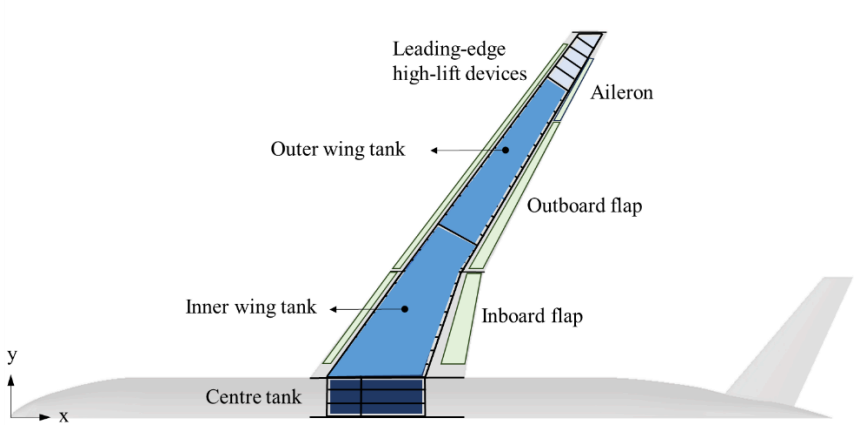
Figure 3. Spanwise discretisation of the CRM wing-box model. The 7-section model groups multiple rib-bounded boxes into larger sizing regions, whereas the 33-section model sizes each rib-bounded section independently.

3.4 Structural idealisation and inertial modelling

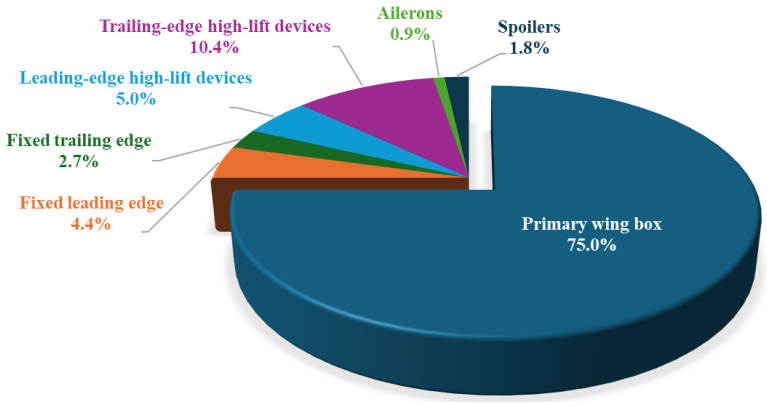
The present study focuses on the composite CRM wing configuration. The structural idealisation follows the SLoT–SAIT modelling approach described in detail in [8]. In summary, the skin covers, spar webs, and rib webs are represented using an intermediate-modulus carbon/epoxy composite laminate, while the spar caps, stringers, rib flanges, and web stiffeners are modelled using aluminium-alloy T-section idealisations. This representation provides an efficient preliminary model of the stiffened semi-monocoque wing box while retaining the main load-carrying and stiffness characteristics required for structural and aeroelastic assessment. During sizing, the skin and web thicknesses, stringer dimensions, and stringer pitch are adjusted to minimise structural mass while satisfying the strength, buckling, fatigue, and aeroelastic constraints defined in Section 3.3. The resulting spanwise mass and stiffness distributions are then used for static deformation, gust-response, modal, and flutter analyses.

Secondary structural masses, fuel, and engine effects are included to improve the representativeness of the preliminary model, as shown in Figure 4. The secondary structures include leading-edge and trailing-edge devices, control surfaces, and associated non-primary components. These are estimated using empirical mass methods and distributed along the span. Fuel is represented as a distributed inertial mass in the wing tanks, while engine effects are included both as localised structural loads and, for aeroelastic analysis, as a lumped mass at the pylon location. This distinction allows the local sizing influence of engine loads to be separated from the global aeroelastic influence of engine mass.

https://doi.org/10.71945/icas2026_0628



(a) Schematic layout of secondary structures and fuel tanks.



(b) Mass breakdown of the wing structure.

Figure 4. Representation of secondary structural components, fuel distribution, and engine/pylon location used in the preliminary sizing and aeroelastic assessment [8].

4 Load-Case and Constraint Definition

4.1 Load case definition

A reduced set of representative load cases was selected to support preliminary composite wing sizing and criticality assessment. In detailed aircraft design, a large number of manoeuvres, gust, ground, landing, and localised loading conditions must be considered. However, such an exhaustive load set is not practical for early multidisciplinary design optimisation, where many structural configurations may need to be assessed rapidly. The aim here is therefore not to reproduce a full certification load analysis, but to identify a compact set of cases that captures the dominant internal load paths and governing structural constraints.

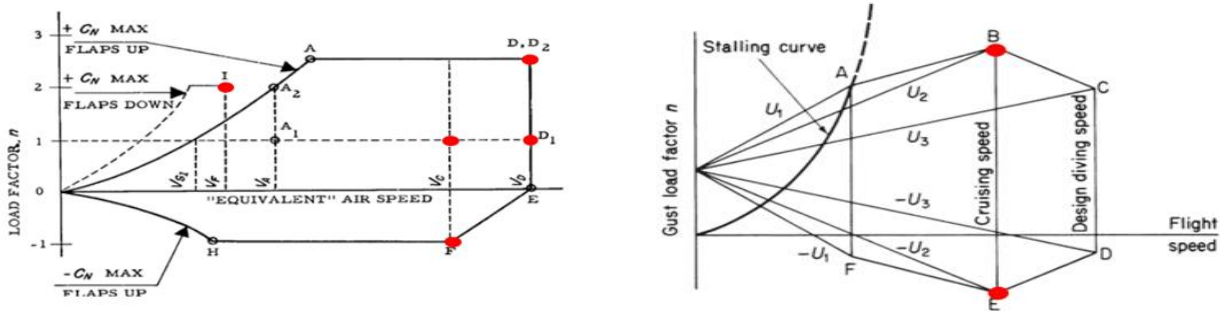
Fifteen representative load cases were defined for the CRM wing, as summarised in Table 2. These include cruise, buffet, symmetric pull-up, symmetric push-down, flap-down, rolling manoeuvre, discrete gust, and engine-induced loading conditions. The aerodynamic cases were selected with reference to typical transport-aircraft manoeuvre and gust envelopes, consistent with preliminary interpretation of CS-25/FAR Part 25 requirements. Ground and landing-gear-related cases were not included because the current wing-box model does not include a landing-gear structural representation. The selected aerodynamic load cases include cruise flight, critical manoeuvres (e.g., pull-up, push-over, and roll), landing scenarios (particularly with flaps deployed), and gust conditions, based on the typical flight and gust envelopes illustrated in Figure 5. The red points in the figure indicate the selected design load cases listed in Table 2. As shown in the gust envelope, the maximum gust load factor occurs at the cruising speed, VC.

Table 2. Load cases applied for structural sizing of the wing (VC is design cruise speed; VD is design dive speed; VFE is maximum flap-extended speed).

Load Case ID	Load type	Description	Details
1	Aerodynamic	Cruise	37000 ft, 1.0 g symmetric, VC

https://doi.org/10.71945/icas2026_0628

2	loads	Buffet	37000 ft, buffet (reference Ma = 0.89 [16])
3		Cruise	Sea level, 1.0 g symmetric, VC
4		Symmetric pull-up	Sea level, 2.5 g symmetric pull-up, VD
5		Symmetric pull-up	Sea level, 2.5 g symmetric pull-up (reference Ma = 0.64 [16])
6		Symmetric push-down	Sea level, -1.0 g symmetric push-down, VC
7		Flap down at landing	Sea level, 2.0 g flap down 40 degrees, VFE
8		Rolling manoeuvres	Sea level, Aileron +/-25 degrees, VD
9		Discrete gust	Sea level, VC
10			37000 ft, VC
11	Engine loads	Engine max load at cruise	6.5 g vertical + 1.5*max cruise thrust
12			-3.5 g vertical + 1.0*max cruise thrust
13		Engine max load at take-off	3.0 g vertical + 3.0*max take-off thrust
14			3.0 g vertical + 3.0*reverse thrust
15		Engine max side loads	+/- 3.0g side



(a) Typical Part 25 load cases and standard transport V-N diagram of FAR25.33.

(b) Typical gust envelope.

Figure 5. Flight and gust envelopes with selected design load cases (from CRM website) [17].

For the aerodynamic load cases, spanwise loading was calculated using the aerodynamic tools available within the SLoT framework. The ESDUpac A95010 lifting-surface method was used as the primary aerodynamic tool, supported by comparison with strip-theory estimates and higher-fidelity or alternative methods, including Cranfield VFP and AVL. The aerodynamic loads were generated under a rigid-wing assumption and then integrated along the span to obtain shear force, bending moment, and torque distributions for structural sizing.

The initial load-envelope assessment showed that the symmetric pull-up cases produced the largest positive shear, bending moment, and torque demands, while the push-down case provided the dominant negative loading condition. These internal load distributions formed the basis for the subsequent composite wing-box sizing and sensitivity study.

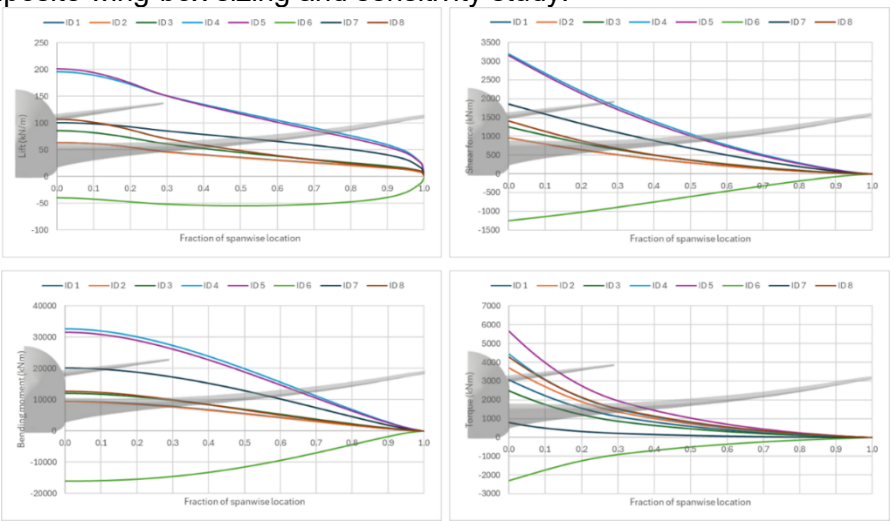


Figure 6. Spanwise aerodynamic and internal load envelopes obtained from the selected manoeuvre

https://doi.org/10.71945/icas2026_0628

cases.

4.2 Sizing criteria and constraint definition

The structural sizing process enforces strength and buckling requirements as the primary design constraints. Strength constraints are evaluated using the maximum stress criterion and the Tsai–Wu failure criterion, applied with a reserve factor of 0.8. Compliance is assessed by monitoring the peak stresses in each composite panel during the sizing process. Damage strain tolerance is also imposed by requiring that the critical strain under ultimate loads does not exceed 3500 $\mu\varepsilon$. For buckling, the structure must remain stable at the limit load with a buckling factor greater than 1.2. Buckling analysis of the stiffened composite skin panels is performed using the finite strip method described in ESDU 03001 [18], supplemented by the practical design guidelines of Niu [19].

In accordance with CS-25 airworthiness requirements, the aeroelastic constraint specifies that the flutter speed V_f must exceed 1.15 times the dive speed V_D. A fatigue criterion is also applied to the skin design. The 1.0g cruise load case is scaled by a factor of 1.3 to account for gust effects, forming the basis of the fatigue design loads. For the CFRP model, a critical fatigue stress threshold of 1000 N/mm² is adopted, based on fatigue strength tests [20], [21].

4.3 Criticality-identification process

To identify the most influential load cases and constraints, a structured sensitivity sequence was applied, as shown in Table 3. Sensitivity steps used for load-case and constraint criticality identification.. The baseline case used the conventional 2.5 g symmetric pull-up manoeuvre with strength constraints only. Additional constraints and load effects were then introduced progressively, including buckling, aeroelastic constraints, wing-box inertial loads, secondary structural mass, fuel mass, fatigue, push-down loading, flap-down loading, rolling manoeuvres, and engine-induced loads.

Table 3. Sensitivity steps used for load-case and constraint criticality identification.

Step No.	Load Case and Description	Design constraints
1	Load Case ID-5 (2.5 g, without inertial loads)	Strength (stress-based)
2	Load Case ID-5 (2.5 g, without inertial loads)	Strength + buckling + aeroelastic
3	Load Case ID-5 (2.5 g, add wing box inertial loads)	Strength + buckling
4	Load Case ID-5 (2.5 g, add inertial loads of wing box, LE&TE, fuel tank)	Strength + buckling
5	Load Case ID-3 (1.0 g with 1.3 load factor for fatigue)	Strength + buckling + fatigue
6	Load Case ID-6 (-1.0 g)	Strength + buckling
7	Load Case ID-7 (2.0 g, flap-down loads)	Strength + buckling
8	Load Case ID-8 (rolling manoeuvre loads)	Strength + buckling
9	Load Case ID-13 (critical engine loads)	Strength + buckling + aeroelastic

Each step generated a new sized wing model. The resulting models were compared in terms of structural mass, spanwise thickness distribution, wingtip deflection, elastic twist, modal behaviour, gust response, and flutter speed. A load case or constraint was considered globally critical if it significantly affected total mass, global stiffness, deformation, or flutter margin. It was considered locally critical if it drove reinforcement in a specific wing region, such as near the engine/pylon attachment or high-lift-device region.

This approach allows the criticality of each load case to be judged by its effect on the final sized structure, rather than by nominal load magnitude alone. The outcome is a prioritised set of governing load cases and constraints suitable for preliminary MDO sizing.

https://doi.org/10.71945/icas2026_0628

5 Results and Discussion

5.1 Baseline sizing and effect of model resolution

The baseline sizing study was first conducted using the 2.5 g symmetric pull-up condition. Both the 7-section and 33-section composite wing-box models were sized under the same loading and constraint assumptions to assess the effect of spanwise discretisation on preliminary mass and stiffness prediction. As shown in Figure 7, the resulting total masses of the two models were close, with the 7-section and 33-section models giving approximately 8172 kg and 8088 kg, respectively. This difference of about 1% indicates that both models capture the dominant global load-carrying behaviour of the wing under the baseline manoeuvre case.

Although the total mass predictions are similar, Figure 7 also shows important differences in the spanwise sizing distributions. The 7-section model produces stepwise thickness distributions because several rib-bounded wing boxes are grouped into larger design regions. In contrast, the 33-section model allows each wing-box segment to be sized independently, giving a more refined representation of local thickness and stiffness variation.

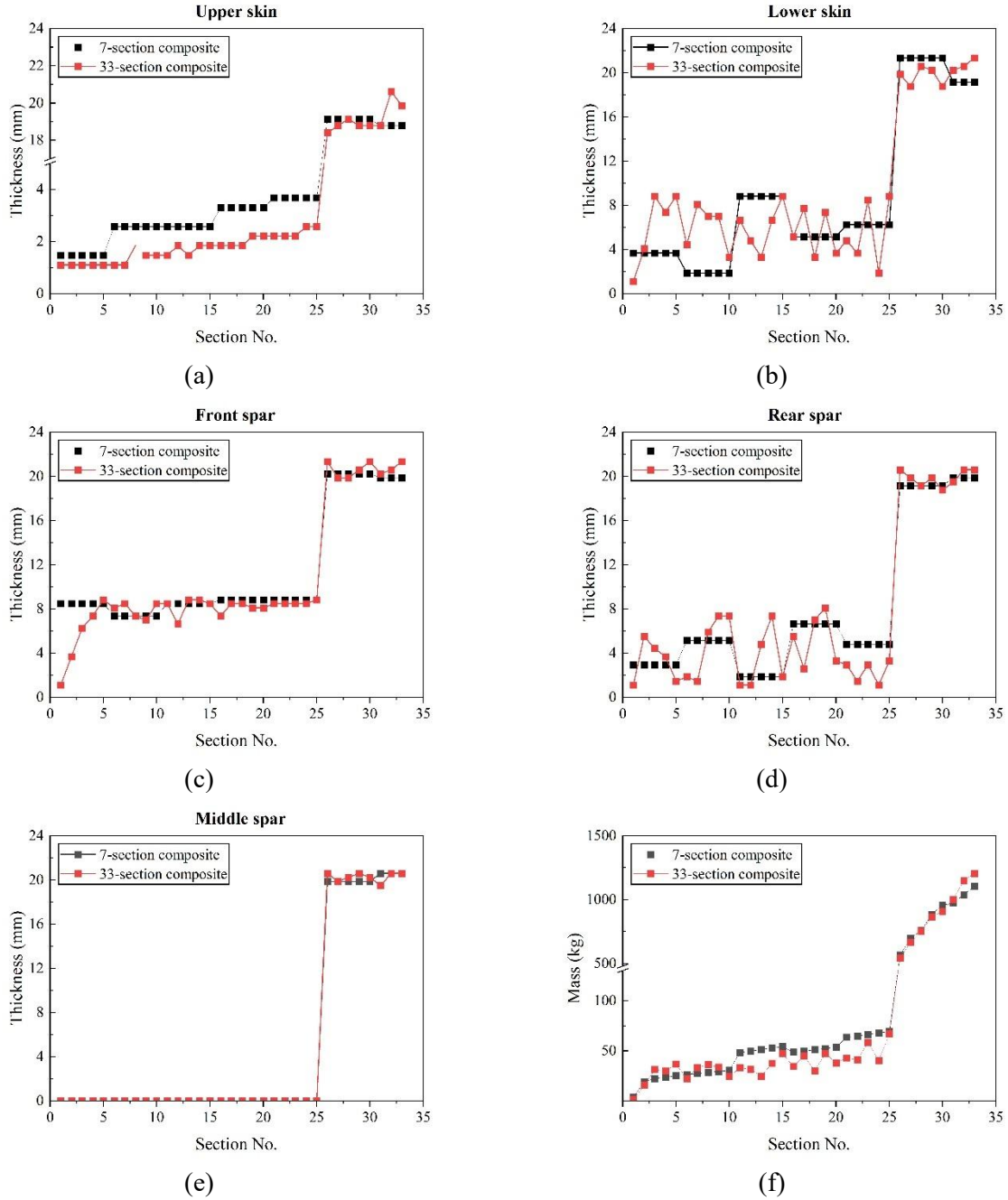
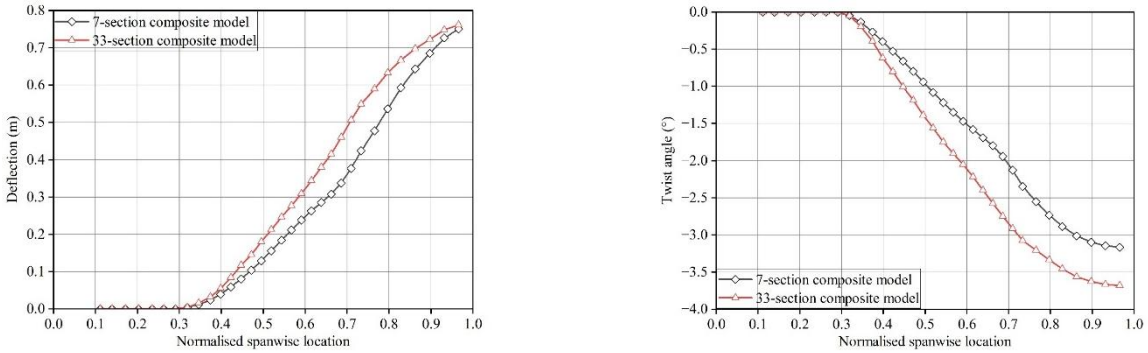


Figure 7. Comparison of spanwise thickness and mass distributions for the 7-section and 33-section

https://doi.org/10.71945/icas2026_0628

composite wing-box models under the baseline 2.5 g sizing condition.

The static response under the same load case is shown in Figure 8. Both models predict similar global bending behaviour, with comparable wingtip deflections. However, the predicted elastic twist differs more noticeably, indicating that torsional stiffness is more sensitive to spanwise discretisation than bending stiffness. This suggests that the coarse 7-section model is useful for rapid global mass estimation, while the refined 33-section model is more appropriate when local stiffness distribution, twist prediction, and load-path interpretation are important.



(a) Deflection (b) Elastic twist angle

Figure 8. Comparison of the static behaviour along the wingspan of the 7-section and 33-section composite models under a 2.5g load.

5.2 Effect of load cases and constraints on structural mass

The sensitivity study was then used to determine how the inclusion of additional constraints and load cases affects the predicted structural mass. Figure 9 compares the mass variation across the sensitivity-study steps for spanwise discretisation. The baseline strength-only case provides the lightest structure, but it does not include the stability and aeroelastic requirements needed for a realistic preliminary design. When buckling and aeroelastic constraints are introduced, the required panel thickness and stiffness increase. This confirms that strength-only sizing is insufficient for composite wing-box design, where thin-walled panel stability can be a governing requirement.

As shown in Figure 9, the inclusion of wing-box inertial loads, secondary structural masses, and fuel mass further modifies the sizing. These effects increase the realism of the preliminary model by representing the distributed inertia associated with the wing structure, high-lift devices, control surfaces, and fuel tanks. Although the corresponding mass increase is moderate, the resulting structure provides improved stiffness and aeroelastic margins.

Figure 9 also shows that the lower-load manoeuvre cases, including the 1.0 g fatigue case, the -1.0 g push-down case, the flap-down case, and the rolling case, affect the sized structure differently. The fatigue case is important because it introduces a repeated-loading constraint that can increase local panel thickness. The flap-down case is more bending-dominated, while the rolling case produces a stronger torsional response. These cases therefore influence different aspects of the structural design, even when they do not produce the largest total wing mass.

Engine-induced loads represent a more localised design driver. As seen in Figure 9, when critical engine loads are applied under the 2.5 g condition, the 7-section model shows a more noticeable mass increase because the coarse design regions force reinforcement over a wider spanwise extent. By contrast, the 33-section model captures the local nature of the engine load path more effectively, limiting reinforcement to the affected region. This demonstrates the importance of refined discretisation when assessing localised load cases.

https://doi.org/10.71945/icas2026_0628

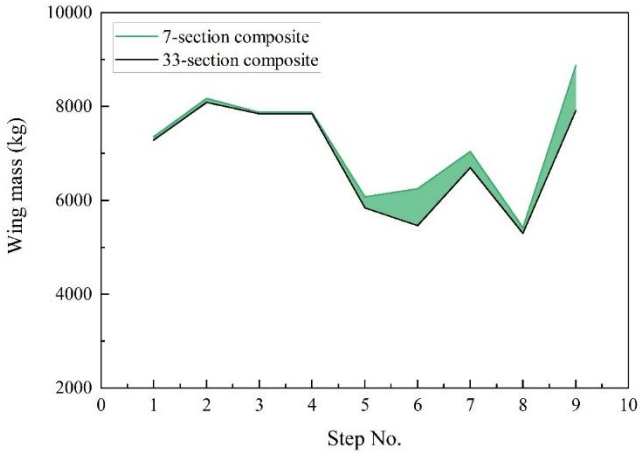
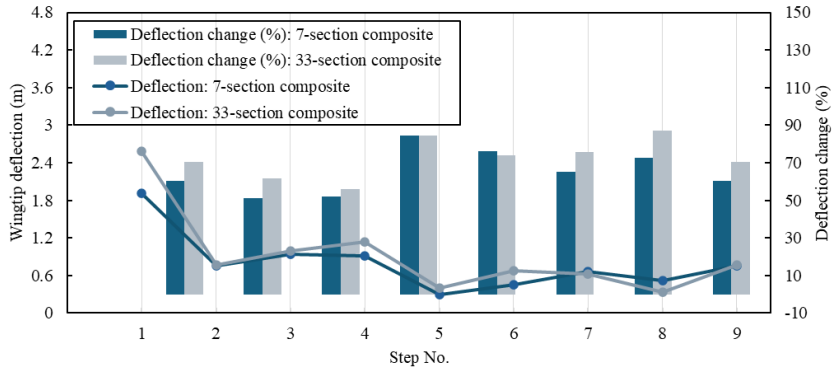


Figure 9. Wing mass variation across the sensitivity-study steps for the 7-section and 33-section composite wing-box models.

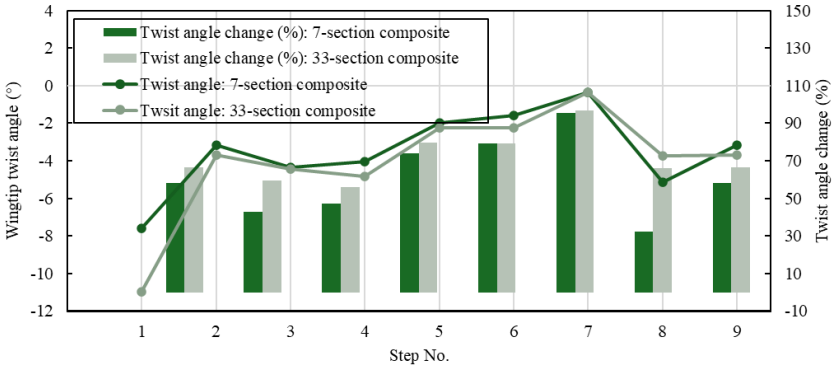
5.3 Effect on static, gust, and aeroelastic response

The structural response of each sized model was assessed using spanwise deflection and elastic twist. Figure 10 shows the variation in wingtip deflection and elastic twist across the sensitivity-study steps. As additional constraints are introduced, particularly buckling and inertial effects, both deflection and twist generally decrease. This indicates that the added constraints drive an increase in bending and torsional stiffness. The most significant stiffness increase occurs when buckling is included under the 2.5 g load condition, confirming that buckling is a dominant design constraint for the composite wing-box structure.

The comparison in Figure 10 also shows that different load cases govern different response quantities. The flap-down load case produces a primarily bending-driven response, while the rolling manoeuvre generates the largest elastic twist. Engine loads have comparatively limited influence on global static deformation, since their effect is concentrated around the engine/pylon region. Therefore, engine loads are locally important for structural reinforcement but do not strongly alter the overall bending and twist response of the wing.



(a)



(b)

Figure 10. Wingtip deflection and elastic twist variation across the sensitivity-study steps.

https://doi.org/10.71945/icas2026_0628

Gust-response analysis was performed to assess the dynamic deformation of the sized wing under representative discrete gust inputs. The gust-response results, shown in Figure 11, indicate that the 7-section and 33-section models produce similar wingtip response trends, suggesting that the global bending response is reasonably well captured by both discretisation. The largest dynamic wingtip deflection occurs at sea level for the longest gust-gradient case considered. Although the gust-induced deformation does not govern the present baseline sizing, Figure 11 shows that gust response remains an important consideration for future applications involving higher-aspect-ratio or more flexible wing configurations.

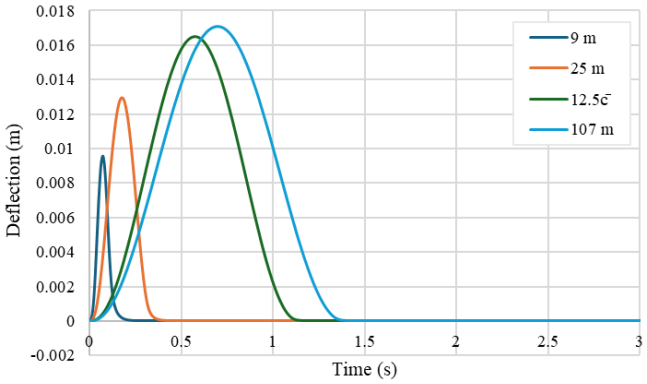


Figure 11. Dynamic wingtip response under selected discrete gust inputs.

Flutter analysis provides a clearer distinction between structural loading effects and mass-distribution effects. Figure 12 shows the flutter speed variation across the sensitivity-study steps. Including buckling, inertial loading, secondary components, and fuel effects generally increases structural stiffness and improves flutter margin. However, the inclusion of engine lumped mass has the opposite effect. Although the engine structural loads have limited influence on global static deformation, Figure 12 shows that the concentrated engine mass significantly changes the modal characteristics and reduces the predicted flutter speed. This demonstrates that engine mass and location must be represented explicitly in preliminary aeroelastic sizing.

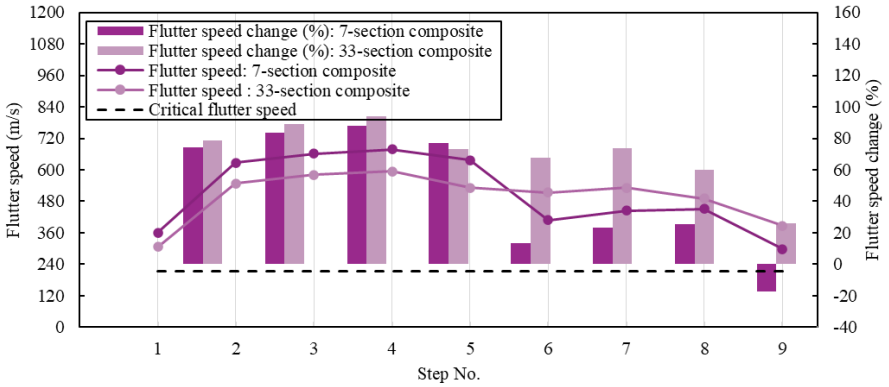


Figure 12. Flutter speed variation across the sensitivity-study steps, showing the influence of buckling, inertial effects, and engine mass representation.

5.4 Critical load-case and constraint interpretation

The results in Figure 7–Figure 12 show that the criticality of a load case cannot be judged from load magnitude alone. The conventional 2.5 g symmetric pull-up case remains important because it defines the dominant positive bending and torsional load envelope. However, the comparison in Figure 9 shows that a strength-only application of this case does not provide a sufficiently representative preliminary design. Buckling must be included because it strongly affects composite panel thickness, global stiffness, and flutter margin. Fatigue also contributes to local panel sizing and should be retained in the preliminary constraint set.

The engine-related cases are critical in a different way. Figure 9 shows that engine structural loads mainly affect local reinforcement around the engine/pylon region and are therefore sensitive to model resolution. Figure 10 shows that the lumped engine mass is globally important for aeroelastic behaviour

https://doi.org/10.71945/icas2026_0628

because it changes the modal characteristics and reduces flutter speed. This distinction highlights the need to separate local structural criticality from global aeroelastic criticality.
The comparison between the 7-section and 33-section models in Figure 7–Figure 10 indicates that the coarse model is adequate for rapid screening of global trends such as total mass and overall bending behaviour. However, the refined model is preferable for identifying local load-driven reinforcement, torsional stiffness variation, and aeroelastic sensitivity. For preliminary MDO, a practical approach is therefore to use the coarse model for early structural layout exploration and the refined model for load-case screening, constraint ranking, and verification of candidate sizing designs.
Overall, the governing design inputs for the present composite CRM wing are the 2.5 g pull-up manoeuvre, buckling constraints, fatigue loading, secondary and fuel inertia, and engine mass representation. The flap-down and rolling cases are important for checking bending- and torsion-dominated responses, respectively, while gust response should be retained for future studies involving more flexible or higher-aspect-ratio wings.

6 Conclusion

This paper presented a methodology for identifying critical load cases and governing constraints for preliminary composite wing sizing using rapid structural and aeroelastic design tools. The approach was demonstrated using a composite wing-box model based on the NASA Common Research Model, with both coarse 7-section and refined 33-section spanwise discretisation considered.
A representative set of aerodynamic, gust, and engine-induced load cases was defined to support preliminary sizing. Rather than treating load criticality purely in terms of applied load magnitude, the proposed approach assessed each case according to its effect on the final sized structure. The resulting models were compared in terms of structural mass, spanwise sizing distribution, static deflection, elastic twist, gust response, modal behaviour, and flutter speed.
The results show that sizing based only on a conventional 2.5 g symmetric pull-up strength case is insufficient for reliable preliminary composite wing design. Buckling constraint become the most critical for strength requirement, leading to thicker sizing parameters and increased structural mass. Secondary structure and fuel inertia primarily affect stiffness behaviour and aeroelastic response. Engine structural loads mainly act as local sizing drivers, whereas the lumped engine mass has a significant influence on modal characteristics and flutter speed. Therefore, engine mass and location should be represented explicitly when assessing aeroelastic stability. The proposed criticality-identification process provides a practical route for reducing the load-case set used in preliminary multidisciplinary design optimisation while retaining the main structural and aeroelastic design drivers. Future work will extend the methodology to more flexible and higher-aspect-ratio wing configurations, where gust response and aeroelastic effects are expected to become more critical. The approach will also support the development of reduced load-case sets for rapid MDO studies involving broader planform, power system and installation, material, and structural-layout variations.

7 Acknowledgements

This research was supported by the Out of Cycle Next Generation Highly Efficient Air Transport (ONEheart) project, funded through UK Research and Innovation under grant number UKRI10003388. The authors would like to thank Airbus Operations Limited UK for their support and cooperation.

8 Contact Author Email Address

Mailto: mushfiqul.alam@cranfield.ac.uk

9 Copyright Statement

The authors confirm that they, and/or their company or organization, hold copyright on all of the original material included in this paper. The authors also confirm that they have obtained permission, from the copyright holder of any third-party material included in this paper, to publish it as part of their paper. The authors confirm that they give permission or have obtained permission from the copyright holder of this paper, for the publication and distribution of this paper as part of the ICAS proceedings or as individual off-prints from the proceedings.

References

[1] Department of Transport, “Jet Zero strategy: delivering net zero aviation by 2050,” London, Jul.

2022.
[2] Directorate-General for Mobility and Transport, “Flightpath 2050 Europe’s Vision for Aviation,” Luxembourg, 2011.
[3] “Certification Specifications (CSs) / Detailed Specifications (DSs) | EASA.” Accessed: Jun. 10, 2026. [Online]. Available: https://www.easa.europa.eu/en/document-library/certification-specifications/group/cs-25-large-aeroplanes
[4] “eCFR :: 14 CFR Part 25 -- Airworthiness Standards: Transport Category Airplanes (FAR Part 25).” Accessed: Jun. 10, 2026. [Online]. Available: https://www.ecfr.gov/current/title-14/chapter-I/subchapter-C/part-25
[5] C.-Y. N. Michael, *Airframe Structural Design: Practical Design Information and Data on Aircraft Structures*. 2002.
[6] K. K. Chawla, *Composite Materials: Science and Engineering*. 2019. doi: 10.1007/978-3-030-28983-6.
[7] J. R. Wright and J. E. Cooper, *Introduction to Aircraft Aeroelasticity and Loads: Second Edition*. 2015. doi: 10.1002/9781118700440.
[8] Y. Pan, M. Alam, J. Whidborne, and M. Westwood, “Rapid preliminary aircraft wing sizing for metallic and composite structures to support data-driven multidisciplinary design optimisation frameworks,” *Aerosp. Sci. Technol.*, vol. 177, p. 112250, Oct. 2026, doi: 10.1016/j.ast.2026.112250.
[9] “NASA Common Research Model (CRM) DPW6 Geometries,” WordPress. [Online]. Available: https://commonresearchmodel.larc.nasa.gov/geometry/dpw6-geometries/
[10] D. Hue, F. Sartor, I. Petropoulos, and C. Fournis, “DPW-7: Steady and Unsteady Computations of the Common Research Model at Different Reynolds Numbers,” *J. Aircr.*, vol. 60, no. 6, pp. 1857–1871, Nov. 2023, doi: 10.2514/1.C037231.
[11] B. K. Stanford and S. J. Massey, “Uncertainty quantification of the FUN3D-predicted NASA CRM flutter boundary,” in *58th AIAA/ASCE/AHS/ASC Structures, Structural Dynamics, and Materials Conference, 2017*, 2017.
[12] Y. Pan, M. Alam, A. Spinelli, and E. B. Aldana, “Structural And Aeroelastic Optimization of A Large Aircraft Wing With A Passive Twist Wingtip,” in *ICAS Proceedings*, 2024.
[13] D. Hue, F. Sartor, I. Petropoulos, and C. Fournis, “DPW-7: Steady and Unsteady Computations of the Common Research Model at Different Reynolds Numbers,” *J. Aircr.*, vol. 60, no. 6, pp. 1857–1871, Nov. 2023, doi: 10.2514/1.C037231.
[14] O. Dababneh, T. Kipouros, and J. Whidborne, “Application of an Efficient Gradient-Based Optimization Strategy for Aircraft Wing Structures,” *Aerospace*, vol. 5, no. 1, p. 3, Jan. 2018, doi: 10.3390/aerospace5010003.
[15] T. R. Brooks, G. K. Kenway, and J. R. R. A. Martins, “Undeflected Common Research Model (uCRM): An Aerostructural Model for the Study of High Aspect Ratio Transport Aircraft Wings,” in *35th AIAA Applied Aerodynamics Conference*, Reston, Virginia: American Institute of Aeronautics and Astronautics, Jun. 2017. doi: 10.2514/6.2017-4456.
[16] T. R. Brooks, G. K. W. Kenway, and J. R. R. A. Martins, “Benchmark aerostructural models for the study of transonic aircraft wings,” *AIAA Journal*, vol. 56, no. 7, pp. 2840–2855, 2018, doi: 10.2514/1.J056603.
[17] N. C. R. Model, “Common Research Model (CRM) Wingbox Finite Element Models.” [Online]. Available: https://commonresearchmodel.larc.nasa.gov/wp-content/uploads/sites/7/2014/02/CRM_wingboxFEM_description_1.pdf
[18] Engineering Science Data Unit (ESDU), “ESDU 03001 Elastic buckling of long, flat, symmetrically-laminated (AsBoDf), composite stiffened panels and struts in compression,” 2003.
[19] M. C.-Yung. Niu, *Airframe structural design : practical design information and data on aircraft structures*. Conmilit Press, 1999.
[20] S. Song, H. Zang, N. Duan, and J. Jiang, “Experimental research and analysis on fatigue life of carbon fiber reinforced polymer (CFRP) tendons,” *Materials*, vol. 12, no. 20, 2019, doi: 10.3390/ma12203383.
[21] N. Morita, Y. Mino, N. Yoshikawa, and M. Hojo, “Versatile fatigue strength evaluation of unidirectional CFRP specimen based on micro-stress analysis of resin,” *Composite Structures*, vol. 276, no. December 2020, p. 114539, 2021, doi: 10.1016/j.compstruct.2021.114539.